Experimental Study of Surface Hardening of AISI 420 Martensitic Stainless Steel Using High Power Diode Laser

Moradi, M., Fallah, M. M. & Jamshidi Nasab, S.

Author post-print (accepted) deposited by Coventry University's Repository

Original citation & hyperlink:
Moradi, M, Fallah, MM & Jamshidi Nasab, S 2018, 'Experimental Study of Surface Hardening of AISI 420 Martensitic Stainless Steel Using High Power Diode Laser', *Transactions of the Indian Institute of Metals*, vol. 71, pp. 2043–2050. https://doi.org/10.1007/s12666-018-1338-4

DOI https://doi.org/10.1007/s12666-018-1338-4
ISSN 0972-2815
ESSN 0975-1645

Publisher: Springer

The final publication is available at Springer via http://dx.doi.org/https://doi.org/10.1007/s12666-018-1338-4

Copyright © and Moral Rights are retained by the author(s) and/ or other copyright owners. A copy can be downloaded for personal non-commercial research or study, without prior permission or charge. This item cannot be reproduced or quoted extensively from without first obtaining permission in writing from the copyright holder(s). The content must not be changed in any way or sold commercially in any format or medium without the formal permission of the copyright holders.

This document is the author's post-print version, incorporating any revisions agreed during the peer-review process. Some differences between the published version and this version may remain and you are advised to consult the published version if you wish to cite from it.

Experimental Study of Surface Hardening of AISI 420 Martensitic Stainless Steel Using High Power Diode Laser

Mahmoud Moradi[1, 2], Mohammad Meghdad Fallah[3], Saied Jamshidi Nasab[1, 2]

1- Department of Mechanical Engineering, Faculty of Engineering, Malayer University, Malayer, Iran

2- Laser Materials Processing Research Center, Malayer University, Malayer, Iran

3- Shahid Rajaee Teacher Training University, Lavizan, Tehran, Iran, P. O. Box: 16785-163.

Abstract

In this paper laser surface hardening of martensitic stainless steel AISI 420 is conducted using a 1600 Watts semiconductor diode laser. Focal plane position, laser power and scanning speed were considered as process variables. Microhardness was measured in depth and surface of the hardened layer and metallography of samples was conducted in order to study the microstructure of hardened zone. Macrography was also performed to measure the geometrical dimensions of hardened zone (width and depth). Microstructure evaluation investigated through optical microscopy and field emission scanning electron microscopy (FE-SEM). Microstructure observation of laser treated zone indicated that the higher surface hardness created the finer and more uniform martensitic phase. Results show that by increasing the laser power and decreasing the focal plane position, depth of penetration and microhardness of hardened zone increase. By increasing the scanning speed and focal plane position, penetration depth decreases while width of hardened zone increases. In desired conditions resulting from this research (laser power 1400 W, scanning speed 5 mm/s and focal plane position 65 mm), surface hardness of AISI 420 martensitic steel increased to 720 Vickers from 210 Vickers obtained. The dimension of hardened layer was 1.2 mm in depth and 6.1 mm in width. Comparing the results with the furnace hardening heat treatment show that the laser hardening process is more effective and precise that conventional processes.

Keywords: Laser surface hardening, High Power Diode Laser, Microhardness, Heat treatment, AISI 420 martensitic stainless steel.

1- Introduction

There are common heat treatment methods for improving surface hardness of steels such as induced and flame heat treatment. The research trend is improving the precision of the processes using modern technologies like laser surface treatment [1]. Recently laser material processing is used for several industrial applications such as laser welding and brazing [2-7], laser drilling [8], and laser cutting [9]. Diode high power laser which is commonly applied in industry could be used for high accuracy surface treatment of the parts.

Martensitic stainless steels are commonly used in manufacturing components employed specially in high stress and corrosion condition. These alloys are used in power plant and petrochemical industry as corrosion resistance components [10]. Steel grade 420 is a martensitic stainless steel that has corrosion resistance similar to 410 plus increased strength and hardness, so it is also used as turbo compressor blades in power plant industry. For increasing the surface hardness of the components it is necessary performing the process with selected laser parameters. These parameters are depend on the laser source type, material specification and desired surface properties. While performing the process on martensitic steel parts, the surface hardness improves through transforming the ferrite and austenite phases to martensitic phase in near surface of the part [11]. In the literature there are several studies achieving the proper input parameter of surface laser hardening process for different materials. Mahmoodi et.al [12] studied the surface hardening of AISI 420 using pulsed Nd:YAG laser and geometry of hardened layer were investigated. Also the corrosion resistance of this steel after laser treatment was evaluated in their work. Lo et al. [13] worked on ND:YAG laser hardening of martensitic stainless steel 440C and concluded that this process could be three times more successful than furnace heat treatment methods. Kim et al. [14] performed the surface hardening of carbon steel using ND:YAG laser. According to their work, increasing the power and scanning speed lead to increasing the depth of hardness. Soriano et al. [15] measured the residual stress and mechanical properties of surface hardened austempered ductile iron and recommended the ND:YAG laser method for this material processing. Badkar et.al [16] studied the effects process parameters in laser surface hardening of pure titanium using Nd:YAG laser. Li et. al [17] investigated the surface hardening process of AISI 1045 using high power diode and CO2 laser. According to their work, performing the process using diode laser would result in higher quality than CO2

one. Bien et.al [18] studied the surface treatment of C80U steel by CO2 laser considering pulse change in designed time ranges. Telesang et .al [19] studied the wear and corrosion behavior of AISI H13 tools steel after performing surface hardening process. Pinahin et al. [20] presented the appropriate process for increasing wear resistance and mechanical behavior of several hard alloys using pulsed laser hardening. Babu et al. [21] investigated the effect of process parameters on microstructure and surface hardness of EN25 steel. They improved the surface hardness of the material two times more than base metal. Moradi et al. [22] presented a research in which the effect of laser pulse energy and focal point position on laser surface hardening of AISI 410 stainless steel studied. Bojinovic et.al [23] simulated the laser hardening process and studied the temperature distribution on an austenitic stainless steel regarding the process parameters. Cordovilla et.al [24] analyzed the surface laser hardening of AISI 4140 steel using FEM. Their method validated by performing experimental tests considering the process overlap tracks.

In the literature the diode laser surface hardening of AISI 420 steel have not been addressed before. In this work the effect of laser process parameters like power, scanning speed and focal plane position studied in the surface hardening process of AISI 420. The resulted hardened layer of pieces measured in depth and width and the microhardness evaluated in selected locations. Also the microstructure evolution studied after performing the process using optical microscope (OM) and FESEM.

2- Experimental Work

In the present work AISI 420 martensitic stainless steel with the chemical composition Table 1 is studied as the work material. The disk shape samples with thickness of 10 mm and diameter of 75 mm were machined and grinded. Figure 1 shows the schematic of the laser surface hardening process.

Table 1. Chemical composition of AISI 420 stainless steel (Wt. %)

Element name/ Wt. %	C	Si	Ni	Mn	P	S	Cr	Mo	Al	V	Fe
AISI 410 stainless steel	0.20	0.50	0.08	0.51	0.034	0.005	12.49	0.01	0.002	0.02	Balance

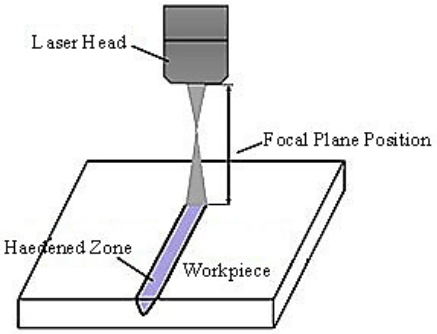

Fig.1. Schematic of the laser surface hardening process

In the experiments a 1600 W diode laser was used for surface hardening of samples. Experimental settings and results of laser hardening process are shown in Table 2. As shown, the ranges of the input variables are: Laser power (1000 – 1600 W), scanning speed (5-7 mm/s) and focal plane position (60-75 mm).

Table 2. Experimental settings and results

Test No	Input Parameters			Output Results		
	Scanning Speed (mm/s)	stand-off distance (mm)	Laser Power (W)	Maximum Hardness (HV)	Depth of hardness (mm)	Width of hardness (mm)
1	5	65	1400	720	1.2	6.1
2	5	75	1400	250	0.51	7.33
3	5	65	1000	478	0.77	6.7
4	7	65	1000	300	0.7	6.5
5	7	70	1600	375	1	6.2
6	6	70	1200	300	0.53	7.2
7	6	60	1200	800	1.3	5.1

Figure 2 shows the images of AISI 420 hardened samples. The numbers written on the samples in Figure 2 are the test number #1 to #7 according to Table 2. The hardened samples were cut in the middle of the process line. To prepare the metallurgical samples, cut specimens were mounted, polished and etched in the vilella's reagent (C6H3N3O7 2gr, Hcl 5cc, C2H5OH 100cc).

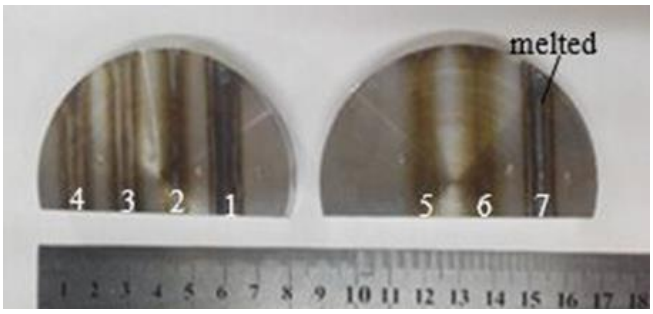

Fig. 2. Image of laser hardened samples for test conditions #1 to #7

The cross section geometry (width and depth) of the hardened zone was measured using BUEHLER MET B7 optical microscope and Image software. Figure 3 shows the schematic of hardened zone measured geometry.

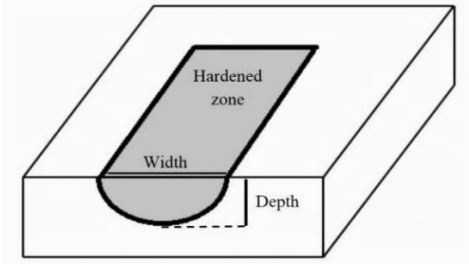

Fig. 3 Cross section of laser hardened zone

The microhardness was measured at least three times for each sample in the depth and width of laser affected zone of sample sections using a micro indentation tester (BUEHLER, USA). The hardness profiles in the laser affected zone along the depth and width directions were plotted for each sample and compared.

3- Results and discussion

In this work the effect of laser power, scanning speed and focal plane position in laser surface hardening of AISI 420 steel was studied. The studied result was dimensions of hardened layer, microhardness distribution in laser affected zone and hardened area microstructure.

3-1- Microhardness distribution

In Figure 4 the cut section of a sample is shown. For each sample, the microhardness was measured in the depth and width of hardened zone.

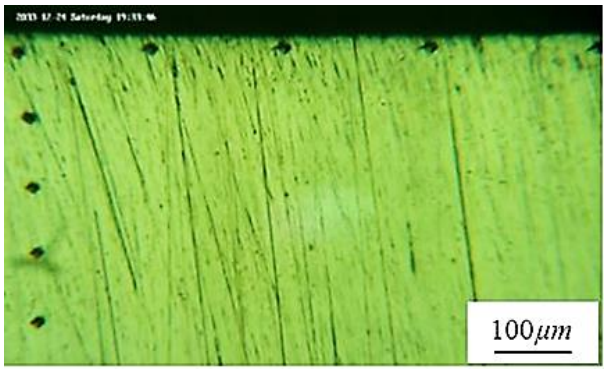

Fig. 4 Cross-sectional view of Vickers indenters in depth and surface of hardened zone

Heat input [9] in laser materials processing is used for better understanding of the process. It could be calculated using Equation (1).

Heat input = Laser power / Scanning Speed (1)

Therefore by increasing the laser power and decreasing the cutting speed, heat input increases and more area of the material will be heated. For Figure 5 and 6, by using this heat input equation, sample #5 has 228.6 J/mm and sample #6 has 200 J/mm when the FPP is the same. Therefore it is obvious that when sample #5 has more heat input, the depth of hardness and maximum hardness will be more than sample #6 with lower heat input.

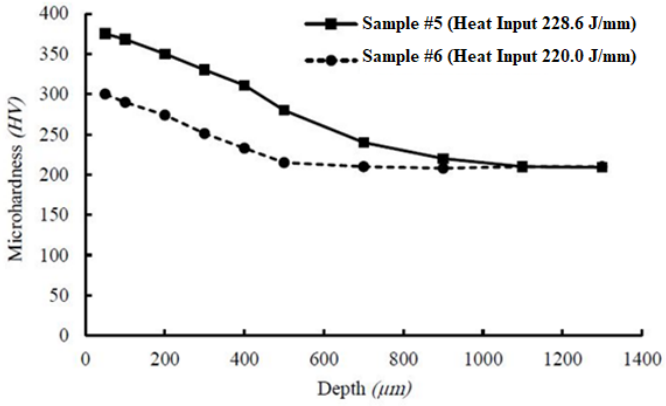

Fig. 5 Microhardness distribution profile in depth of the laser hardened layer (comparison the heat input effect)

Figure 6 shows the distribution of microhardness in half of width in cross section of samples #5 and #6 which processed by heat input 229 and 200 W/mm. In centerline of the sample section that is near to the laser beam, the microhardness is at its maximum value and gradually decreases departing from the centerline. It is crystal clear that the hardness distribution is like a sinusoidal

function and the hardness is maximum in the center and decreases gradually along the outside of hardened zone. The reason of this phenomena is distribution shape of the laser beam energy. As mentioned before the microhardness value and width of sample #5 is more than sample #6 because of higher heat input.

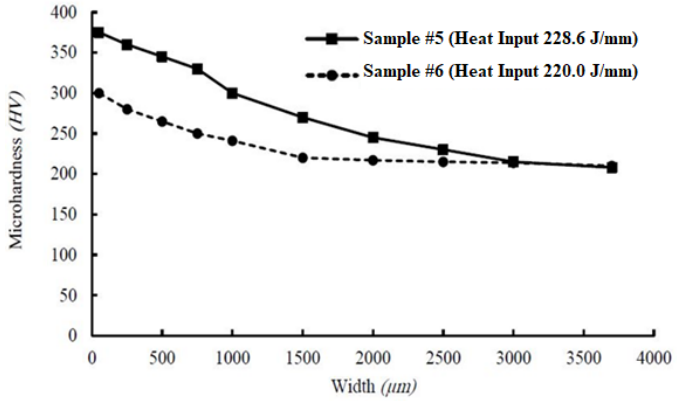

Fig. 6 Microhardness distribution profile in width of the laser hardened layer (comparison the heat input effect)

According to this work, the scanning speed has a direct effect on the process results. By decreasing the scanning speed, the interaction time of the laser beam and heat input energy increase. So, the energy density became higher and the hardness value and its effect area enlarge. In Figure 7, scanning speed of sample #3 is more than sample #4 and so the process is more effective in the former than the latter sample.

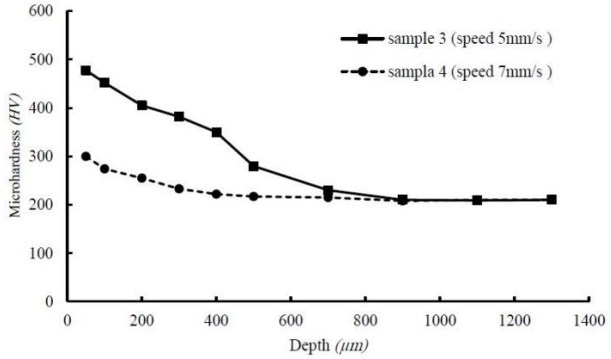

Fig. 7 Microhardness distribution profile in depth of the laser hardened layer (comparison the scanning speed effect)

3-2- Geometrical dimensions of hardened layer

Figure 8 displays the distribution of laser beam energy in the direction of its movement. As illustrated, the focal plane position affects the input energy concentration and geometrical dimension of processed area. Increasing the focal plane position leads to diverging the laser beam and decreasing the energy density while the beam area interact with the material increases.

Focal plane position equal to 60 mm means that the focal plane is above the surface and in this case the red area would be 12 mm^2 (the dimension of the Focal Plane is 8×1.5 mm). The surface which the laser beam interact with the material surface is calculated. It should be explained that the divergence angle of the beam is differ in tow side. In the Fast (1.5 mm) and Slow (8 mm) are 11 and 6 degree, respectively (Table 3).

Table 3. The area of the laser beam interact with the material

Focal plane position **(**mm**)**	Beam Area in interaction with surface material (mm^2)
60	12
65	25.34
70	42.77
75	64.3

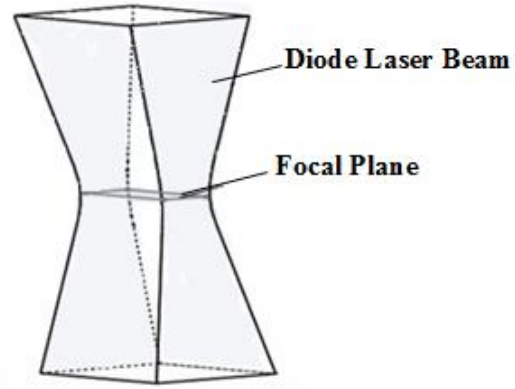

Fig. 8 Schematic of diode laser beam distribution

Figure 9 shows the microhardness value and its depth for samples #1 and #2 with 65 mm and 75 mm focal plane position respectively. As the focal plane position rises, the maximum hardness and penetration depth reduces but the affected width increases.

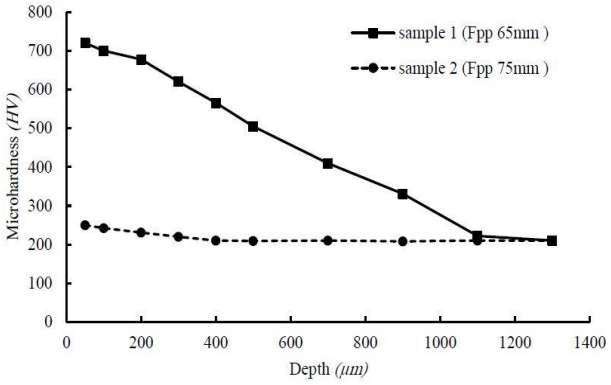

Fig. 9 Microhardness distribution profile in depth of the laser hardened layer (comparison the focal plane position effect)

For measuring the geometrical dimensions of laser affected area, the macrographic examination of samples carried out which are shown in Figure 10 for samples #1, #3 and #7 after grinding, polishing and etching procedure.

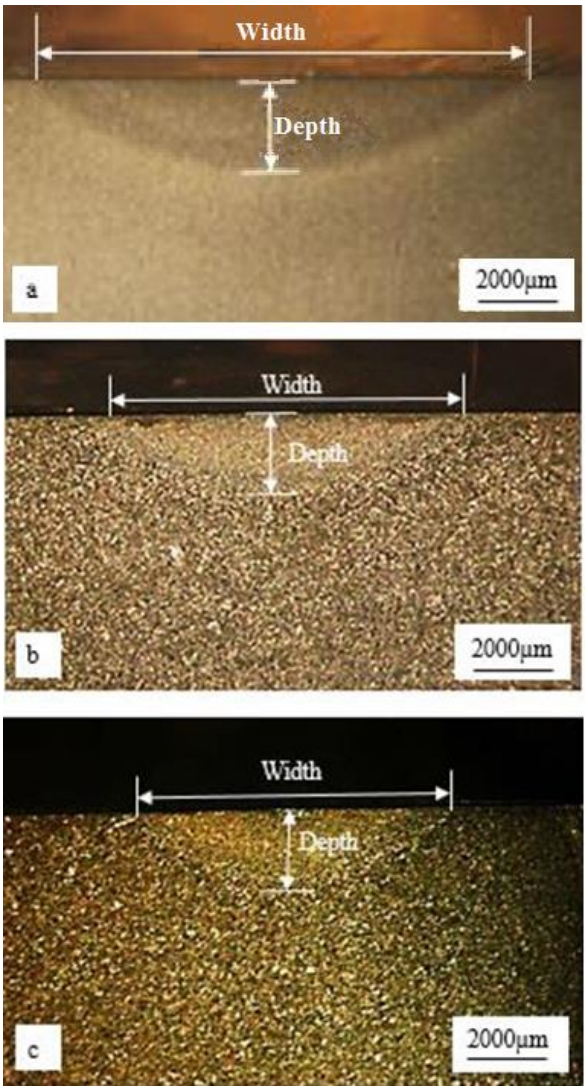

Fig. 10 Cross section of laser hardened samples a) sample # 1 b) sample # 3 c) sample # 7

According to Tables 2 and comparing samples #1 and #2, by increasing the focal plane position from 65 to 75 mm, the depth of hardened zone decreases while the width increases.

3-3- Microstructure of hardened layer

The microstructure of samples studied in this work via metallographic attempts and optical microscopy. Figure 11-a illustrated the microstructure of material before laser processing. It is realized that some ferrite phase is distributed in the base martensitic field. Figure 11-b shows the microstructure of laser processed sample #4 without any ferrite phase in the material.

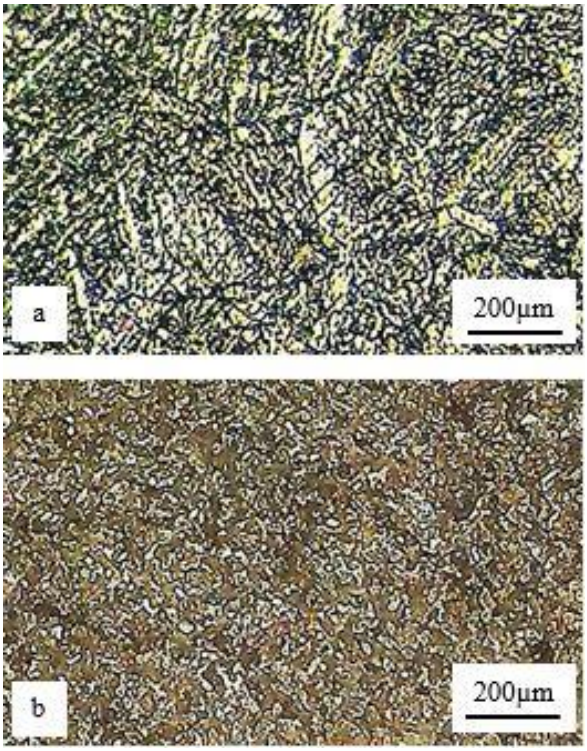

Fig. 11 a) Microstructure of base martensitic stainless steel AISI 420 b) Microstructure of laser hardened metal sample #4

Microstructure of processed samples #1 and #2 are shown in Figure 12 which reveal the full martensitic phase in the microstructure. According to investigations, increasing the heat input energy in the process via using higher laser power, lower scanning speed and lower focal point position distance leads to increasing the austenite phase temperature and finally decreases the austenite grain sizes. Also it is evidence that by controlling the scanning speed, the uniformity of grains could be achieved.

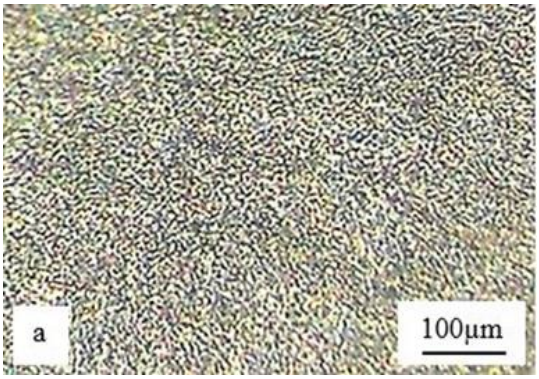

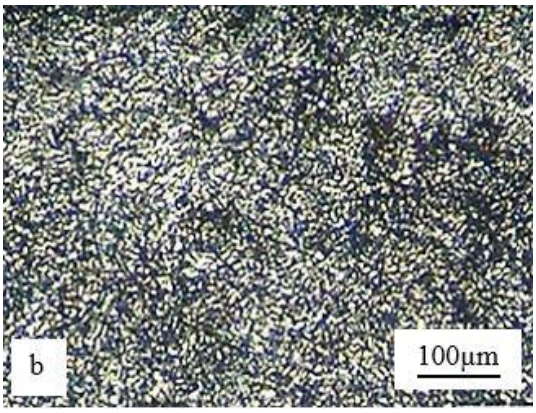

Fig. 12 Microstructure of laser hardened zone of martensitic steel AISI 420 a) sample #1 b) sample #2

FESEM images of base material and laser hardened sample #1 are shown in Figure 13. According to Figure 13-b, the carbide particles are completely fined and distributed in the structure while the ferrite phase dissolved and declined in size. In the microstructure of base metal (Figure 13-a), the laminated and spherical carbides exist in the grain boundaries and grains, respectively. In the laser processed material, the laminated carbides dissolved in the grain boundaries while spherical ones remains in the grains as shown in Figure 13-b.

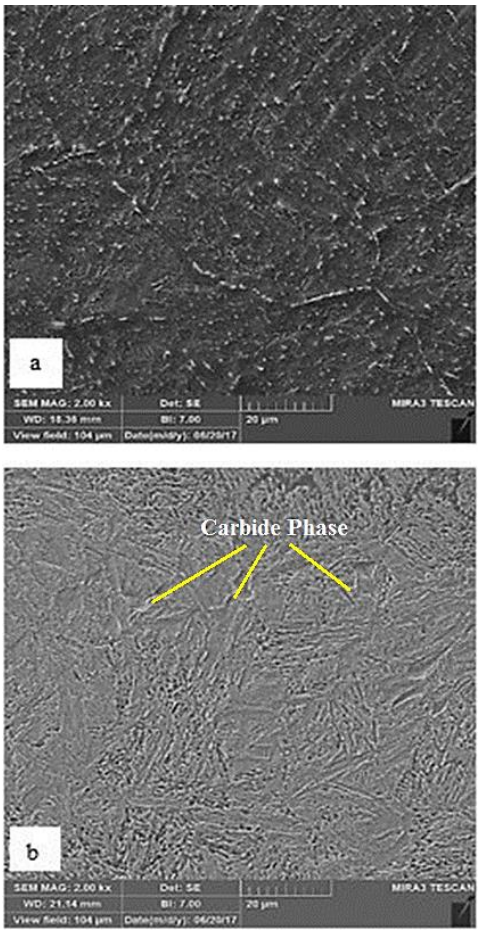

Fig. 13 FESEM image a) base material of AISI 420 b) laser hardened sample # 1

4- Furnace hardening of AISI 420

For comparing the laser surface hardening method with conventional method, the furnace heat treatment according to cycle presented in Figure 14 was conducted. The material preheated to 540 ℃ for 1 hour and heated to 980 ℃ with the rate of 70 ℃/hour and was kept for 2 hour. The samples quenched in oil, water and air and the hardness was reported 528 Vickers, 560 Vickers and 513 Vickers, respectively.

Due to the possibility of micro-crack formation in the water, and the lower the hardness in the air, the oil is an ideal quenching method with a hardness of 528 Vickers for AISI 420. So the hardness value with the diode laser hardening method (800 Vickers) is 1.5 times than the furnace hardening heat treatment. Table 4 shows the comparison of the hardness results of furnace hardening heat treatment and laser surface hardening.

Table 4. Comparison of furnace hardening heat treatment and laser hardening

Heat treatment cycle	furnace hardening heat treatment	laser hardening
Cooling in oil	528 Vickers	-
Cooling in water	560 Vickers	-
Cooling in ear	513 Vickers	-
Laser Surface Hardening	-	800 Vickers

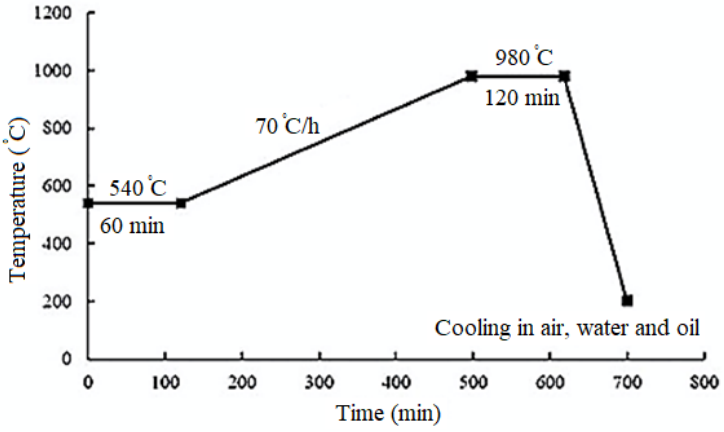

Fig. 14 furnace hardening heat treatment cycle of AISI 420 used in this research

The microstructure of furnace hardened sample is compared with laser processed sample in Figure 15. The fine carbide particles in furnace processed sample dispersed in the martensitic field. In the laser processed sample due to relatively high cooling rate, these particles are interconnected which causes reducing strength and hardness of the material. For decreasing the ferrite field and overcome the problem, the laser power should select higher and scanning speed should decrease. Also due to high energy concentration, the localized hardness occurred.

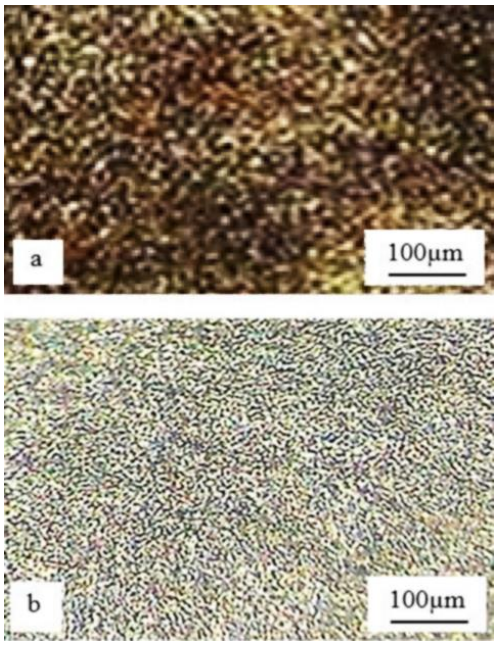

Fig. 15 a) Microstructure of furnace hardening AISI 420 b) Microstructure of laser hardening sample #1

5- CONCLUSIONS

In this work, the effect of laser power, scanning speed and focal plane position are investigated in diode laser surface hardening process of AISI 420. The studied outputs were geometrical dimensions of hardened layer (i.e. width and depth), microhardness values in laser affected area and samples microstructures. According to experimental works, the following results concluded:

1. By increasing the laser power and decreasing scanning speed the heat input increases which leads to increases in the microhardness and geometry of the affected area.
2. Reducing the focal plane distance causes more energy density resulting in increases the depth and microhardness of hardened layer.
3. Increases of microhardness from 210 HV to 720 HV with depth of 1.2 mm and width of 6.1 mm, is possible by using laser surface hardening process of AISI 420 stainless steel.
4. The value of the surface hardness in laser surface hardening process is about 25% more effective than conventional hardening process.
5. Laser surface processing of martensitic stainless steel AISI 420 causes changing initial ferrite phases of the base metal to completely martensitic phase. Also by controlling

the process parameters it is possible to control final product microstructure and uniformity of grains.

6- References

1. Kannatey E, Asibu Jr, *Principles Of Laser Materials Processing*, John Wiley and Sons, New Jersey (2009), p 568.

2. Moradi M, Salimi N, Ghoreishi M, Abdollahi H, and Shamsborhan M, *J Laser Appl* **26** (2014), p 022004.

3. Sundqvist J, Kaplan A F H, Granström J, and Sundin K G, *J Laser Appl* **27** (2015), p 042002.

4. Moradi M, Ghoreishi M, Torkamany M, Sabbaghzadeh J, and Hamedi MJ, *Adv Mat Res* **383** (2012), p 6247.

5. Faraji A H, Moradi M, Goodarzi M, Colucci P, and Maletta C, *Opt Lasers Eng* **96** (2017), p 1.

6. khorram A, Jafari A, and Moradi M, *Modares Mechanical Engineering* **17** (2017), p 129.

7. Moradi M, Ghoreishi M, and Khorram A, *Laser Eng* **39** (2018), p 379.

8. Moradi M, and Golchin E, *Lat Am J Solids Stru* **14** (2017), p 464.

9. Moradi M, Mehrabi O, Azdast T, and Benyounis H Y, *Opt Laser Technol* **96** (2017), p 208.

10. Li L, *Opt Lasers Eng* **34** (2000) p 231.

11. Puli R, and Ram G D J, *Surf Coat Technol* **209** (2012) p 1.

12. Mahmoudi B, Aghdam A R S, and Torkamany M J, *JEST* **8** (2010) p 87.

13. Lo K H, Cheng F T, and Man H C, *Surf Coat Technol* **173** (2003) p 96.

14. Kim J D, Lee M H, Lee S J, and Kang W J, *T Nonferr Metal Soc* **19** (2009) p 941.

15. Soriano C, Leunda J, Lambarri J, Navas V G, and Sanz C, *Appl Surf Sci* **25** (2011) p 7101.

16. Badkar D S, Pandey K S, and Buvanashekaran G, *T Nonferr Metal Soc* **20** (2010) p 1078.

17. Li R, Jin Y, Li Z, and Qi K, *J Mater Eng Perform* **23** (2014) p 3085.

18. Bien A, and Szkodo M, *J Mater Process Tech* **217** (2015) p 114.

19. Telasang G, Majumdar J D, Padmanabham G, and Manna I, *Surf Coat Technol* **261** (2015) p 69.

20. Pinahin I A, Chernigovskij V A, Bracihin A A, and Yagmurov M A, *J Frict Wear* **36** (2015) p 330.

21. Babu P D, Buvanashekaran G, and Balasubramanian K R, *T Can Soc Mech Eng* **36** (2012) p 241.

22. Moradi M, Karami Moghadam M, Zarei J, and Ganji B, *Modares Mechanical Engineering* **17** (2017), p 311.

23. Bojinovic M, Mole N, and Stok B, *Surf Coat Technol* **273** (2015) p 60.

24. Cordovilla F, Garcia-Beltran A, Sancho P, Dominguez J, de-Lara L R, and Ocana J L, *Mater Des* **102** (2016) p 225.